IOP Conf. Series: Materials Science and Engineering **433** (2018) 012069 doi:10.1088/1757-899X/433/1/012069

Removing Pb(II) by means of natural and acid-activated nanoporous clays

Z Ghazizahedi and M Hayati-Ashtiani*

Department of Chemical Engineering, Faculty of Engineering, University of Kashan, Kashan, Iran

*Author to whom correspondence should be addressed. Email: hayati@kashanu.ac.ir

Abstract. Heavy metals such as Pb(II) are harmful to both the environment and human health as they are both toxic and stable. Bentonite clays contain Montmorillonite, which is a nano-porous and nano-structured mineral that can act to remove metals. In these experiments, natural bentonite S1 was activated using sulfuric acid solutions under various conditions with a range of Liquid to Solid ratios (L/S), Temperatures (T), Times (t) and Concentrations (C). The activated samples S2 (L/S= 16 mL/g, T= 95 °C, t= 4 h, C=5 M) and S3 (L/S= 16 mL/g, T= 95 °C, t= 6 h, C=0.5 M) showed the highest and the lowest amounts of Pb(II) removal, respectively. The characterisation of natural and acid-activated bentonites in terms of Pb(II) separation applications were examined using Transmission Electron Microscopy (TEM), X-Ray Diffraction (XRD), X-Ray fluorescence (XRF), Brunauer-Emmett-Teller (BET) surface area measurements, and Fourier Transform Infrared Spectroscopy (FTIR). Metal removal experiments were conducted using a suspension of 0.3 g suspended in 25 mL $Pb(NO_3)_2$ solution under fixed solution concentrations of 2,000 mg/L. The suspensions were thoroughly mixed for 24 hours at 250 rpm. The results showed the removal capacities of samples followed the order of S2 > S3 > S1, and suggested that the prevailing Pb(II) removal processes were adsorption and ion exchange.

1. Introduction

Bentonite clays, which contain montmorillonite as their dominant mineral, are hydrated 2:1 type aluminium silicates that contain an alumina octahedral layer sandwiched between two tetrahedral layers of silica in a nanocrystalline structure [1], [2]. Bentonites are used in many industrial applications, including in bleaching processes, as dispersants in drilling fluids and cements, in cosmetics, and in paints [3], [4]. One of the important applications of bentonites is metal adsorption, which is very useful in many industries, as it acts to remove heavy metals such as lead, zinc, nickel, uranium, copper, cobalt, and cadmium.

The existence of toxic heavy metals in industrial activities has become an important environmental concern. Lead (Pb) is one of the most fatal poisonous metals that regularly enters the environment, arising from various preliminary sources and industrial, metallurgical, mining, jewellery, tanning, chemical, electrical, and electronic activities [5], [6], [7], [8]. Certain heavy metals, including lead, can be dangerous to aquatic animals and plants, as well as being easily absorbed into the human body, and as such they are a prime cause of illnesses in humans such as anaemia, muscular cramps, kidney malfunction, nausea, renal degradation, skeletal deformity, and cardiovascular diseases [8], [9].

Many technologies have been developed to remove toxic heavy metals from solutions in recent decades, including ultrafiltration, reverse osmosis, chemical precipitation, solvent extraction, electro dialysis, oxidation, reduction, ion exchange and adsorption [8], [10]. Adsorption has been proved to be

one of the best methods for removing toxic heavy metals such as lead, as it is an economical and feasible method in most situations. Bentonites act as adsorbents for the removal of lead, and they are low-cost, have low hydraulic conductivity, are hydrophilic, and have micro-porous structures which have high adsorption capacities useful in the separation process for lead [7], [8], [9], [10], [11].

Bentonite is one of the most frequently chosen low-cost adsorbents for the removal of heavy metals. Bourliva et al. (2015) studied the adsorption of metal systems by bentonites and showed that the adsorption capacity of bentonite for Pb(II) was 85.47 mg g^{-1}, demonstrating that bentonite displayed high selectivity toward Pb(II). A compacted mixture of bentonite has also been proposed as a buffer or backfill material for the disposal of high-level radioactive waste as bentonites are stable to irradiation [12]. Chen et al. showed that moisture quickly travelled through a bentonite/sand mixture infiltrated with Pb(II) solutions and that the amount of bentonite content influenced Pb(II) retention. The amount of bentonite present can be determined through a combination of the instrumental and experimental tests [13]. Nithya and Sudha studied the removal of Pb(II) using chitosan-g-poly(butyl acrylate)/bentonite, with the bentonite acting to improve the stability of chitosan. Adeyemo et al. and Khalfa et al. found in their works that acid activation improved the adsorption capacity of bentonites in dyes and Cr(IV) [14], [15]. Chemical modification such as acid-activation is one of the best techniques to improve the physicochemical properties of bentonites in terms of removing Pb(II), and is thus discussed in this paper.

The aim of this study is to determine the best bentonite sample for removing Pb(II) through a combination of laboratory and instrumental tests on currently-used bentonite samples from different regions of Iran. The new approach seeks new insights into the characterisation of these specific samples and aims to interpret the specific results to gain an understanding of the physio-chemical properties of bentonites for the separation of Pb(II). The selectivity to Pb(II) of nanoporous clay is also investigated. The novelty of this work is the study of the Pb(II) separation process using a combination of laboratory and instrumental tests.

2. **Material and methods**

2.1. Materials and treatments

Natural bentonite, S1 (from deposits of Mahrijan, Isfahan, Iran), and two acid-activated forms were studied. Lead(II) nitrate ($Pb(NO_3)_2$, 99.5%) and sulfuric acid (H_2SO_4, d=1.84, 95-98%) were purchased from Merck Chemicals.

2.2. Sampling, drying and ball-milling treatment

The commercial natural bentonite chunks were air dried and ground on site. Then, the bentonite was sent to the laboratory where the natural sample was further oven dried at 110 °C overnight and ground using a ball mill. The sample was powdered to less than 1.19 mm particle size (Sieve Mesh No. 16) for the acid activation process.

2.3. Acid activation of bentonite

Homogeneous suspensions of the bentonite sample with a liquid/solid ratio 16 mL/g (50 gr Bentonite in 800 mL liquid) were prepared in which the 800 mL liquids had various concentrations of 0.5, 1, 1.5, 2, 3, 4, 5, 6, 7, and 8 M of sulfuric acid (H_2SO_4, d= 1.84 and 95-98% purity) mixed at 95 °C in a four-necked 2-L glass reactor. The suspensions of bentonite in H_2SO_4 solutions were mixed for 2, 4, and 6 hours. At the end of the acid-activation process, the suspensions were filtered and washed with distilled water to achieve an SO_4^{2-} ion-free filtrate. The activated samples were then dried in an oven at 110 °C for 16 hours and ground to pass through a 200-mesh (75 μm) sieve.

The best and worst Pb adsorption results were obtained for S2 (L/S= 16 mL/g, T= 95 °C, t= 4 h and C=5 M) and S3 (L/S= 16 mL/g, T= 95 °C, t= 6 h and C=0.5 M), respectively.

2.4. Pb removal procedure

To show the Pb adsorption capacity of bentonites, batch experiments were conducted using suspensions of 0.3 g absorbent in 25 mL of Pb(NO3)2 solution in distilled water with the solution concentration

fixed at 0.01 N. The suspensions were thoroughly mixed in a shaker (GALLENKAMP, England) for 24 hours at 250 rpm in 100-mL-polyethylene-capped bottles to eliminate the effects of the 24-hour equilibrium time. The bottles and glassware were washed with distilled water; this was followed with an acetone wash and the vessels were dried before use.

Separation was accomplished using a filter paper and vacuum pump setup. A filtrate was used to determine the amount of adsorbed Pb along with ICP (Spectra AA200 model, Varian Corp., Victoria, Australia) adsorption tests using an air-acetylene flame. Analytical calibration was made with aqueous standards 2, 5, 10, and 20 ppm of Pb(II) from a 1,000-ppm stock solution.

The values of the distribution ratio in mLg-1 were calculated from eq. 1:

$$K_d = \frac{C_0 - C_{eq}}{C_{eq}} \times \frac{V}{m} \quad (1)$$

where C_0 and C_{eq} are the initial and equilibrium concentrations (mgL^{-1}), V is the aqueous phase volume (mL), and m is the sorbent mass (g).

The adsorption percentage (R) and capacity (Γ) were calculated from eqs. 2 and 3, respectively:

$$\%R = \frac{100 \times K_d}{K_d + \frac{V}{m}} = (1 - C_{eq} / C_0) \times 100 \quad (2)$$

$$\Gamma = K_d \times C_{eq} = (C_0 - C_{eq}) \times V/m \quad (3)$$

where R is the percentage of adsorption, Γ is the adsorption capacity, C_0 is the initial concentration (gmL^{-1}), C is the equilibrium concentration (gmL^{-1}), V is the aqueous phase volume (mL), and m is the adsorbent mass (g).

2.5. XRD analysis

The samples were characterised using X-ray diffraction (XRD) diffractometer (PW 1800, Philips, Netherlands) equipped with a graphite secondary monochromator using Cu–Kα radiation in the 2θ from 2.010° to 50°; the step of 2θ was 0.020°. The samples were first dried and then powdered to less than 75 μm before XRD analysis.

2.6. XRF analysis

X-Ray Fluorescence was carried out using Oxford ED 2000 model equipment (England) along with Xpertease software to determine the chemical changes in the samples.

2.7. BET Surface area and pore size analysis

The specific surface areas and pore size distributions of the natural and acid activated bentonites were measured using a Quantachrom (Nova 2000e, Florida) volumetric N_2 adsorption instrument. The adsorption temperature of N_2 was 77.3 K at relative pressure up to P/P0~0.95. Ambient nitrogen, oxygen, and other gases adsorbed into the surface and open pores of the bentonite samples were completely removed at low pressure and T = 100 °C for 8 hours before any measurements were taken.

2.8. Infra-Red Spectroscopy

IR spectroscopy of the samples was performed using a Fourier Transform Infra-Red (FTIR) spectra in the KBr method. The bands were recorded between 4,000 to 400 cm^{-1} along with a spectral resolution of 4 cm^{-1} and a Bruker (VECTOR 22, Massachusetts) spectrometer instrument was used. A small amount, 1 mg, of each clay sample was mixed with 200 mg of KBr and each mixture was dried at 110℃ overnight in the oven to remove any free water.

2.9. Transmission Electron Microscopy

The morphologies of the natural and acid activated bentonite samples were analysed using a Philips type (EM 2085S, Eindhoven) Transmission Electron Microscope (TEM). Holey carbon-coated grids were applied to prepare the samples, and the maximum electronic accelerator voltage was 100 kV.

3. Results

3.1. Pb removal

Table 1 shows the calculated Pb(II) distribution coefficient, adsorption percentage (adsorption efficiency), and adsorption capacity of samples S1, S2, and S3. The measured parameters allow comparison of the Pb adsorption properties of raw bentonite (S1), and the acid-activated samples (S2 and S3) as listed in Table 1.

Table 1. Distribution coefficient, adsorption percentage, and adsorption capacity of samples.

Sample	Distribution coefficient *(mLg^{-1})*	Adsorption percentage *(Dimensionless)*	Adsorption capacity *(Dimensionless)*
S1	6558	98.74	85
S2	63250	99.86	177
S3	45939	99.82	165

The results demonstrate that the order of distribution coefficient (K_d), adsorption percentage (R) and adsorption capacity (Γ) for these samples is S2> S3> S1.

3.2. XRD analysis

The mineralogical results of natural bentonite (S1), best Acid-activated (S2), and worst Acid-activated (S3) samples (as obtained with XRD) are shown in figure 1. The peaks of montmorillonite (MMT) and quartz (Q) phases are at 2θ, or about 7, 20 and 21, and 26 and 28. Quartz is the major non-clay mineral in all samples, though the quartz peak intensity decreases in S1 and increases in S2.

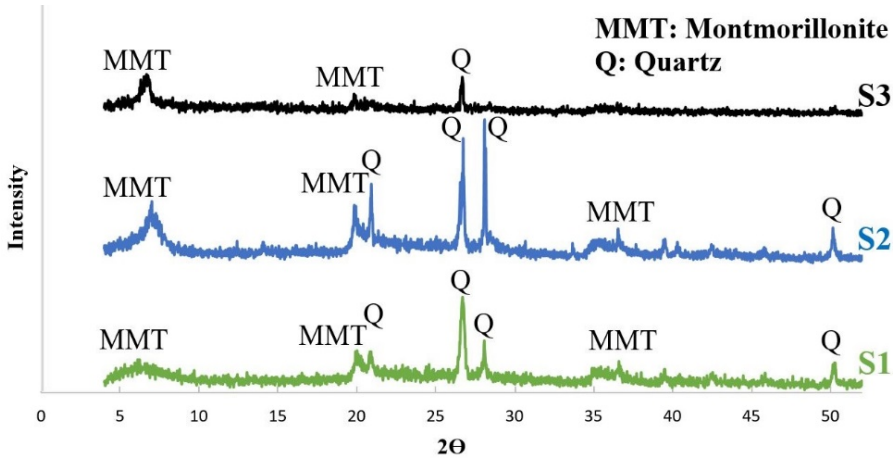

Figure 1. XRD patterns of S1 (natural) and S2 and S3 (acid-activated) samples.*3.3. XRF analysis*

The XRF analysis results of natural (S1), the best Acid-activated (S2) and the worst Acid-activated (S3) samples are given in Table 2. The results indicate that S2 had a higher amount of SiO_2. The amount of Na_2O in S2 and S3 was zero, and S2 and S3 also had lower amounts of MgO and Al_2O_3. The value of CaO in sample S3 was lower than those seen in S1 and S2.

Table 2. The XRD analysis results of the S1 (natural), S2 and S3 (acid-activated).

Analyte (*Wt%*)	Na_2O	MgO	Al_2O_3	SiO_2	K_2O	CaO	TFeO [a]	Others
S1	0.8	1.8	18.3	74	0.2	0.8	2.2	1.9
S2	0.0	1.1	11.2	84.2	0.1	0.9	1.1	1.4
S3	0.0	1.5	17.0	76.9	0.2	0.3	1.8	2.3

[a] TFeO = FeO + Fe_2O_3

3.4. BET surface area and pore size analysis

The specific surface area of the samples was calculated using both single and multi-point BET analysis. The external surface area of the samples was measured using the BET method since the electrically neutral molecules of N_2 could not penetrate into the pores. As Table 3 indicates, S1 and S2 had the minimum and maximum surface areas, respectively.

Table 3. BET surface area (single and multi-point) and pore size analysis (BJH method).

Sample Name	A_{BET} *(m^2/g)* Single Point BET	A_{BET} *(m^2/g)* Multi Point BET	Average Nano Pore Diameter *(nm)* BJH Method
S1	22.2170	22.63	3.613
S2	119.9080	122.4	3.574
S3	70.8544	71.92	3.608

Figure 2 shows the amount of adsorbed nitrogen volume plotted against relative equilibrium pressure. This plot corresponds to type II N_2 adsorption isotherms and type III adsorption-desorption hysteresis.

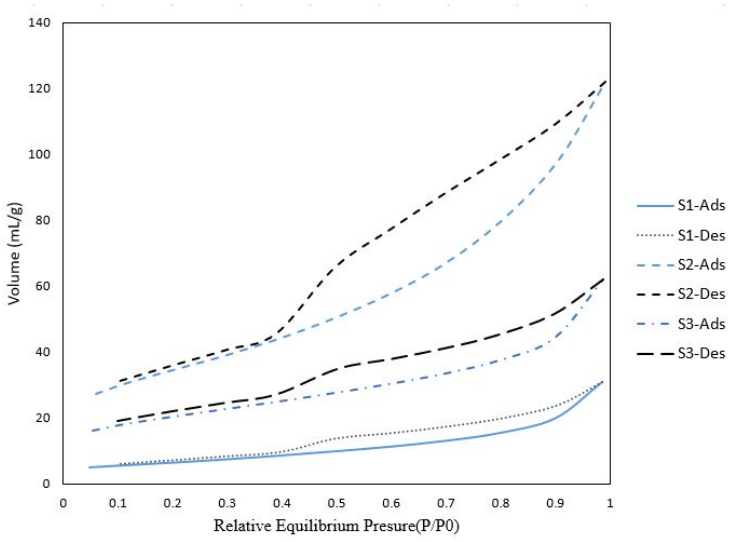

Figure 2. Absorbed nitrogen volume against relative equilibrium pressure.

Bentonites are nano-structured, nano-porous clays. Pore size distribution was obtained using BJH analysis. Bentonite samples have mainly meso and nano pores, and Table 3 shows that S1 had the maximum and S2 the minimum average pore diameter. The plot of pore volume versus pore diameter is shown in figure 3. Increase in pore diameter leads to an increase in volume of adsorbed nitrogen, and

the increasing trend in the amount of adsorption volume of nitrogen for sample S2 is greater than those of S1 and S3.

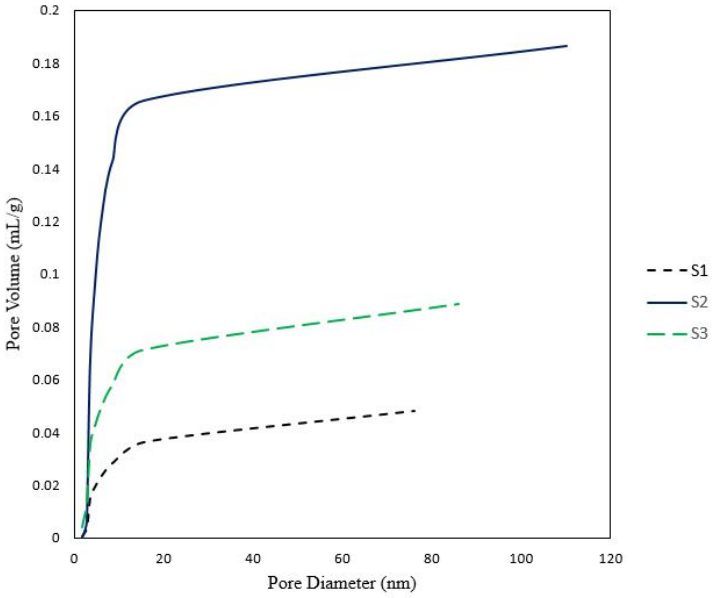

Figure 3. Pore volume versus pore diameter

The BJH analysis in figure 4 shows the diameters of the samples as being between 3 and 5 nm and the pore volumes of samples S1, S2, and S3 were 0.0014, 0.0068, and 0.0025 mL/g, respectively. Sample S2 displayed maximum pore volume.

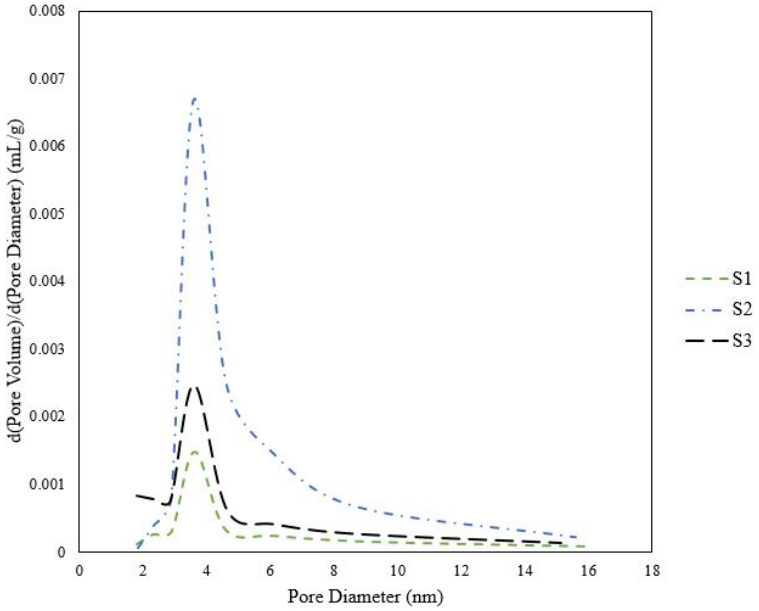

Figure 4. BJH pore diameter analysis of the sample S1, S2 and S3

3.5. Infra-Red Spectroscopy analysis

FTIR is one of the most useful methods for characterising bentonite composition. Table 4 indicates the reference and bands of samples S1, S2, and S3 and figure 5 shows the FTIR curves. The width absorption bands at 3,623 cm^{-1} demonstrate the OH stretching bands of S1, S2, and S3, which are typical for montmorillonite hydroxyl groups coordinated with Al^{3+} cations. The bending mode of Mg•OH•Al and Fe•OH•Al appeared at 3,422 cm^{-1}. Absorption at approximately 1,639 cm^{-1} demonstrates H_2O corresponding to the H•O•H deformation. An Al•Al•OH asymmetric stretching mode appeared at 917 cm^{-1}. The peaks at 793 cm^{-1} were assigned to a platy form of disordered tridymite. The adsorption spectrum at 725 cm^{-1} in the spectrum of montmorillonite suggests the presence of Free or Amorphous Silica. The Al•O•Si bending mode appeared at 524 cm^{-1} and the absorption at 692 cm^{-1} demonstrates the presence of quartz. The peak at 466 cm^{-1} was assigned to Si•O•Si stretching.

Table 4. FTIR band assignments for S1, S2 and S3 and the reference bands.

S1	S2	S3	Assignments	Maxima(cm^{-1})
474	467	458	Si•O•Si Bending	466
527	532	520	Al•O•Si Bending	524
696	696	696	Quartz	692
718	717	-	Free or Amorphous Silica	725
800	800	786	Platy form of Tridymite	793
918	922	917	Al•Al•OH Bending	917
1643	1636	1638	Hydration, OH Bending	1639
3430	3427	3422	OH Stretching, Hydration	3422

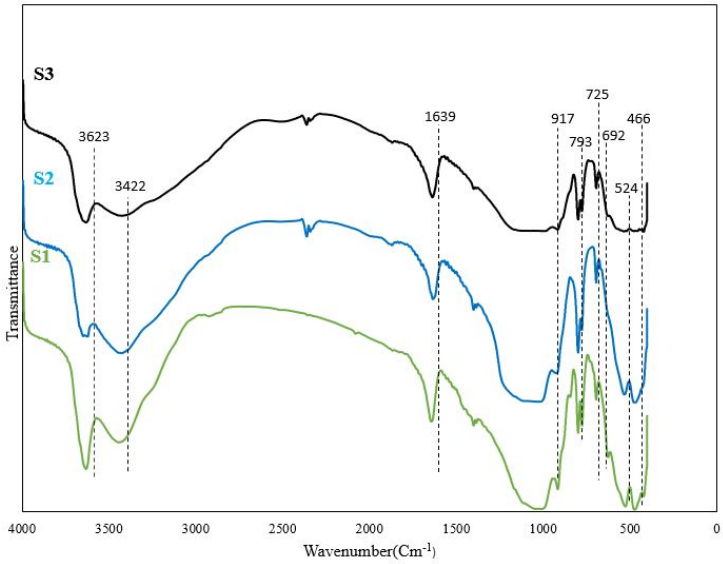

Figure 5. FTIR curves.

3.6. Transmission Electron Microscopy analysis

The morphology and size of the samples were analysed using TEM (figure 6). Figures 6a, 6b, and 6c correspond to samples S1, S2 and S3, respectively. Figure 6 shows that all samples had aggregating particles, though S2 had a smaller particle size than the other samples.

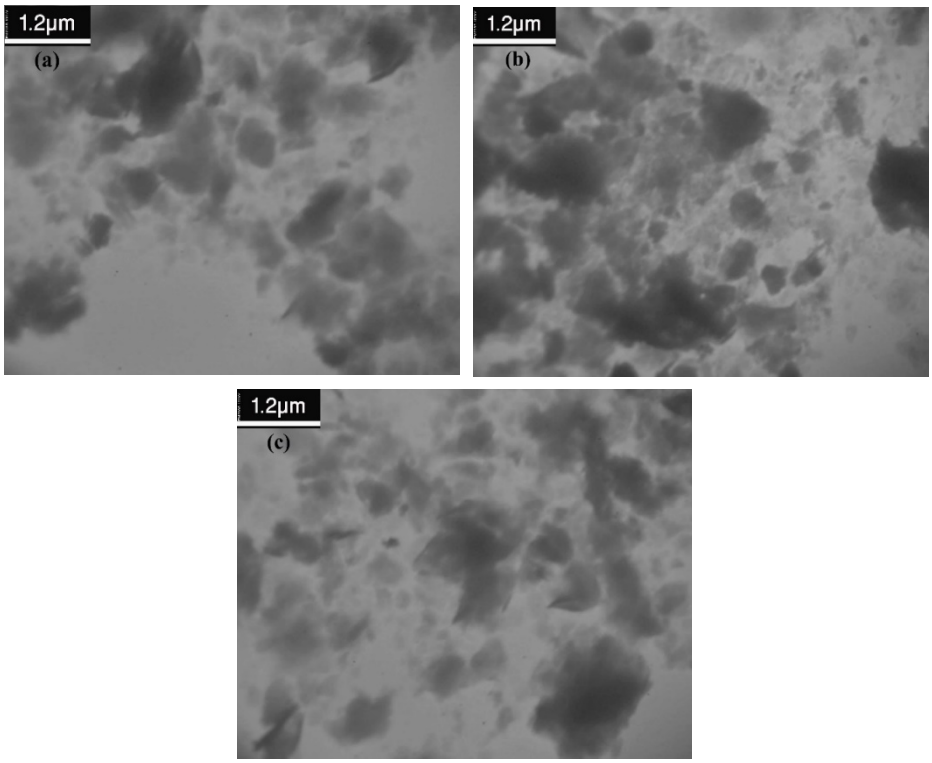

Figure 6. The morphology and size of samples using TEM: (a) S1, (b) S2, and (C) S3.

4. Discussion

The chemical, physical and structural properties of the bentonites are considerably changed by applying bentonite modification methods such as acid activation. The changes include both mineralogical and chemical compositions; surface area and pore size distribution; chemical bonds' shape and structure; and the amount of metal removal, in accordance with the other alterations. The results of the modifications are thus discussed using instrumental analyses, as is the metal removal process.

Figure 1 shows the XRD patterns of S1, S2, and S3. The major diffraction peaks at 2θ, about 7, 20 and 35, demonstrate the montmorillonite and at 2θ about 21, 26, 28, and 50 show the quartz phase. The intensity of montmorillonite and quartz peaks was increased in sample S2 through acid activation compared with S1 and S3, as illustrated in figure 1. The acid activation decreased or eliminated the intensity of some peaks in sample S3, as the quantity of impurities decreased.

The XRF analysis of S1, S2, and S3 samples is given in Table 3. S1 had the maximum amount of Al_2O_3, indicating the highest amount of montmorillonite, as the XRD results showed that there were no other phases with Al_2O_3. The amount of Na_2O in S2 and S3 reached zero because of isomorphic substitution of the Na^+ of montmorillonite with the H^+ of the sulfuric acid. The value of CaO in sample S3 was lower than those in S1 and S2 because the power of acid activation of sample S3 was lower than in S2 and the natural S1.

The FTIR analysis helped to identify the chemical structure of the samples. For the acid-activated samples, S2 and S3, the slight reductions in the peak intensities at 1,639 and 3,422 cm^{-1} correspond to dehydration of OH bending and stretching bands. The significant decline in band intensity at 3,623 cm^{-1} indicates the development of the dehydroxylation process for S3. The intensity of the quartz bending vibration bands at 692 cm^{-1} is almost unchanged in all samples. The decline in absorption band intensities of Si•O•Si, Si•O•Al and Al•Al•OH at 466, 524, and 917 cm^{-1} denote decreases in

montmorillonite amount for sample S3. The amount of SiO_2 increases in response to the decrease in montmorillonite wt%, and the XRF analysis confirms the increase of SiO_2 wt% for S3.

Figure 6 shows the TEM graphs of the submicron-sized plate-like particle morphology of S1. A higher number of finer particles could be observed in S2, however, which has relevance to Pb(II) adsorption, as it makes sample S2 an adsorbent with a higher specific surface area than the other samples.

The adsorption–desorption isotherms of the natural and acid activated samples (figure 2) show a single modal pore size distribution centred at 3.5 nm. Acid activation significantly increased the nano and meso pore size distribution seen in acid-activated S2 and S3 to around 3.5 nm modal. Most of the pores are in the mesopore region. Macropores were also observed for the best-activated sample, S2. The highest surface area of the best acid activated sample was related to the micro and macropores produced after acid activation, and acid activation also increased the number of pores for both activated samples.

The IUPAC classifications of the N_2 adsorption/desorption isotherms of the natural and acid-activated samples indicated that they were type II isotherms, and both activated samples exhibited H3-type hysteresis, including narrow pore size distribution, as shown in figure 2. Type III hysteresis is known to exist in solids consisting of agglomerates or aggregates of particles forming slit-shaped pores (plates or edged particles such as cubes), with no uniform size and/or shape. Hysteresis is usually due to differing behaviours in adsorption and desorption.

Adsorption studies of Pb(II) show that the adsorption ability of natural S1 is lower than that of acid-activated S2 and S3 (Table 1). Amongst the acid-activated samples investigated here, sample S2, which was activated under L/S= 16 mL/g, T= 95 °C, t= 4 h, and C=5 M conditions, had the highest adsorption ability. The intensities of montmorillonite and quartz peaks in the XRD patterns of S2 indicated the highest amount of montmorillonite and the lowest amount of quartz impurities within all samples, aiding Pb(II) removal. The FTIR bands for montmorillonite and quartz confirmed this claim. The results of XRF confirmed the increase in montmorillonite content of S2, as the unsuitable impurities decreased in S2 compared to S3. Figure 6 reveals that S2 had finer particles than the other samples, giving S2 the highest surface area in accordance with BET studies. The single and multi-point BET results show that S2 had 119.9080 and 122.4 m^2/g, respectively. The increased surface area provided additional available sites to adsorb metals. Figure 4 also shows that the numbers of micro, meso, and macro-pores were highest for sample S2. Pb^{2+} diameter is 2.38 nm, which means that the Pb^{2+} cations can be easily adsorbed on internal surfaces or pores of montmorillonites as well as on the external surfaces.

5. Conclusions

Acid-activation of nanoporous bentonites is a convenient, useful, and economical method for removing toxic and harmful heavy metals such as Pb from aqueous solutions. XRD, XRF, BET, FTIR, and TEM results were used to explain the physio-chemical and structural changes in samples to explain the improved adsorption capacities of natural bentonite after acid activation.

The XRD patterns showed that acid activation decreases or eliminates the intensity of impurity peaks. The XRF studies suggested that the amount of Na_2O in S2 and S3 reached zero because of isomorphic substitution of Na^+ in the montmorillonite with the H^+ of the added sulfuric acid. The FTIR study of S3 showed an increase in the amount of SiO_2 after acid activation, which was confirmed by XRF analysis. Adsorption studies of Pb(II) showed that sample S2, which was activated under the L/S= 16 mL/g, T= 95 °C, t= 4 h and C=5 M conditions, had the highest adsorption ability.

Reference

[1] Abdeen Z, 2015 Characterization and Application of Extracted Natural Polymer Fiber (Aminopolysaccharide) as Weight Reducing Agent *Environ. Process.* **2** 189

[2] Simsek S and Ulusoy U, 2012 Uranium and lead adsorption onto bentonite and zeolite modified with polyacrylamidoxime *Radioanal. Nucl. Chem.* **292** 41

[3] Alver B E, Alver Ö, Günal A and Dikmen G, 2016 Effects of hydrochloric acid treatment on structure characteristics and C_2H_4 adsorption capacities of Ünye bentonite from Turkey: a combined FT-IR, XRD, XRF, TG/DTA and MAS NMR study *Adsorption* **22** 287

[4] Yildiz N, Calimli A and Sarikaya Y, 1999 The characterization of Na_2CO_3 activated Kutahya bentonite *Turk. J. Chem.* **23** 309
[5] Dutta J and Mishra A K, 2016 Influence of the presence of heavy metals on the behaviour of bentonites *Environ Earth Sci.* **75** 993
[6] Fernández-Nava Y, Ulmanu M, Anger I, Marañón E and Castrillón L, 2011 Use of granular bentonite in the removal of mercury (II), cadmium (II) and lead (II) from aqueous solutions *Water Air Soil Pollut.* **215** 239
[7] Nithya R and Sudha P N 2016 *Textiles and Clothing Sustainability*. **2**1 8
[8] Rafiei H R, Shirvani M and Ogunseitan O A 2014 Removal of lead from aqueous solutions by a poly(acrylic acid)/bentonite nanocomposite *Appl. Water Sci.* **6** 331
[9] Dlamini D S, Mishra A K and Mamba B B 2012 Adsorption Behaviour of Ethylene Vinyl Acetate and Polycaprolactone-Bentonite Composites for Pb^{2+} Uptake *Inorg. Organomet. Polym.* **22** 342
[10] Bourliva A, Kleopas M, Sikalidis C, Filippidis A and Betsiou M, 2015 Adsorption of Cd(II), Cu(II), Ni(II) and Pb(II) onto natural bentonite: study in mono-and multi-metal systems *Environ. Earth Sci.* **73** 5435
[11] Chen Y, Zhu Ch, Sun Y, Duan H, Ye W, Wu D and Chunming 2012 Adsorption of La(III) onto GMZ bentonite: effect of contact time, bentonite content, pH value and ionic strength *Radioanal. Nucl. Chem.* **292** 1339
[12] Chen Y G, Jia L Y, Ye W M, Wang Q, Chen B and Cui Y J 2015 Infiltration of Pb(II) solution in compacted bentonite/sand mixture under unconfined conditions *Environ. Earth Sci.* **74** 6137
[13] Hayati-Ashtiani M, Jazayeri S H, Ghanadi M and Nozad A 2011 Experimental Characterizations and Swelling Studies of Natural and Activated Bentonites with Their Commercial Applications *J. Chem. Eng. Jpn.* **44** 67
[14] Adeyemo A A, Adeoye I O and Bello O S 2017 Adsorption of dyes using different types of clay: a review *Appl. Water Sci.* **7** 543.
[15] Khalfa L, Cervera M L, Bagane M and Souissi-Najar S 2016 Modeling of Equilibrium Isotherms and Kinetic Studies of Cr (VI) Adsorption into Natural and Acid-Activated Clays *Arab. J. Geosci.* **9** 75